Advances in Computational Design, *Vol. 6, No. 4 (2021) 301-317*
https://doi.org/10.12989/acd.2021.6.4.301

Analyzing dynamic characteristics of nonlocal porous graded beams under impulse and thermal loading

Mouayed H.Z. Al-Toki[1], Raad M. Fenjan[2], Ridha A. Ahmed[2], Nadhim M. Faleh*[2] and Wael Najm Abdullah[2]

[1]*Middle Technical University, Technical College, Baghdad, Iraq*
[2]*Al-Mustansiriah University, Engineering Collage P.O. Box 46049, Bab-Muadum, Baghdad 10001, Iraq*

(Received October 9, 2019, Revised September 12, 2021, Accepted September 19, 2021)

Abstract. In the framework of nonlocal strain gradient theory, the dynamic responses of a porous functionally graded (FG) nano-size beam under half-sine impulse load and thermal environment. The half-sine impulse load has been modeled as a point load located on the top surface of the nano-size beam. The exerted impulse load leads to the transient vibrations of the nano-size beam at a prescribed time. The porous beam has been described with two pore distributions named even-type and uneven-type pores. The formulation has been developed based upon the refined beam model while the equations will be solved numerically using differential quadrature (DQ) method. Finally, the dynamic deflections in transient region will be derived with the usage of Laplace transform technique. It will be indicated that temperature variation, pore distribution and nano-scale factors have remarkable influences on dynamic resonse of the nano-size beam subjected to sine-type impulse loads.

Keywords: ceiling modules; FEM analysis; integrated ceiling; seismic ceiling

1. Introduction

Evaluation of mechanical characteristics of nano-scale structures including nano-size beams and nano-size plates according to non-classic elasticity theories has been a serious case of study in recent decade. The main reason is broad application of nano-scale structures in nano-sensors or nano-electro-mechanical systems (NEMs). The most familiar theories for modeling of nano-scale structures are nonlocal elasticity (Eringen 1983) and strain gradient (Lam *et al.* 2003) theories. In the theories, some scale factors have been introduced in order to interpolate the influences of small size (Kunbar *et al.* 2020, Akgöz and Civalek 2015, Mirjavadi *et al.* 2020a, 2020b, Ahmed *et al.* 2020, Fenjan *et al.* 2021). Pursuant to nonlocal elasticity the stress field is necessary to be nonlocal since the relation between the stress and the strain at a point depends on the strains of that point and also surrounding points (Nami and Janghorban 2014). This nonlocality of stress field has been considered with the use of nonlocal parameter. Any value of nonlocal parameter may be determined using experiment or numerical simulation. However, the derivation of the values of nonlocal parameter based on the mentioned approaches is very difficult and time-consuming.

*Corresponding author, Professor, E-mail: dr.nadhim@uomustansiriyah.edu.iq

http://www.techno-press.org/?journal=acd&subpage=7 ISSN: 2383-8477 (Print), 2466-0523 (Online)

Therefore, many studies on static and dynamic properties of nano-scale structural elements have been performed as parametric studies based on some assumed values for nonlocal parameter (Li *et al.* 2015, Zhang *et al.* 2015, Lou *et al.* 2016).

In recent years, several theoretical studies and experiments report that small size effects must be characterized via stiffness increasing mechanism or strain gradient fields (Martínez-Criado 2016). This assertion is not the same as that of nonlocal elasticity in which stiffness reduction behavior has been stated. However, the influences of reduction and increment on structural stiffness at nano scales can be considered in the context of nonlocal strain gradient theory (NSGT). According to NSGT, two scale factors named nonlocal and strain gradient factors have been utilized to provide an excellent description of small size effects. The static and dynamic properties of nanobeams and other nanostructures have been broadly studied with the use of NSGT (Barati 2018, She *et al.* 2018).

The effects of different loadings on vibration behavior of nanobeams has become an important case of study in recent years. Some of these loadings are harmonic forces, impulsive loads and moving loads at top surface of the nanobeam. Forced vibrations of the nanobeam due to harmonic and impulsive loads have been investigated by several authors in the context of nonlocal elasticity theory (NET) and nonlocal strain gradient theory (NSGT). However, forced vibrations of the nanobeams due to pulse loads has become very important because of the nano-sensing and nano-probing applications (Simsek 2010, Zhang and Liu 2020, Liu *et al.* 2021). It has been realized that the dynamic deflections of a nanobeam due to pule loads increase by the inclusion of nonlocal parameter (Khaniki and Hosseini-Hashemi 2017).

In a FG material, all properties must be described according to the continuous gradation between the two constituents (ceramic and metal). Actually, the mechanical characteristics of a FG material depends on the portion or percentage of each constituent. Therefore, the effective properties of a FG material can be controlled by increasing or reducing the portion of ceramic/metal constituents. Due to excellent properties of FG materials, they have many applications in structures used in aerospace, automobile and civil engineering sections. The distribution of FG material in structures can be mathematically modeled using power-law or Mori-Tanaka models. Using power-law functions, it is possible to easily describe the continuous gradation of material properties with good accuracy, however, Mori-Tanaka scheme has provided more accurate results as reported in some studies. Both models in their traditional forms have ignored the effects of porosities inside FG materials (Atmane *et al.* 2015). The porosities may be created due to some faults during the FG material production and it is shown that they have notable impact in mechanical characteristics of FG structures (She *et al.* 2018, Ahmed *et al.* 2019, El-Hassar *et al.* 2016). In recent years, a modified power-law model has been developed and used by several authors to investigate the mechanical characteristics of FG structures including porosity effects (Mirjavadi *et al.* 2017).

The present research deals with forced vibration behavior of a nanobeam made from porous FG material which is subjected to half-sine pulse load. In this research, the half-sine pulse load is the representative of a point load on the top surface of the nanobeam. A modified power-law model has been used to investigate the dynamic characteristics of FG nanobeams including porosity effects. The nanobeam formulation is based upon higher-order refined beam theory, whereas the size effects have been captured according to NSGT. The governing equations acquired from Hamilton's principle have been solved through DQM and the time domain part of solution has been done using inverse Laplace transform approach. It is exhibited that the moving load speed, nonlocal/strain gradient factors, pore amount, porosity distribution, elastic substrate and graded nonlocality have enormous affection on dynamic response of the nano-sized beams.

2. Theoretical formulation

2.1 Beam modeling via NSGT

As discussed, the influences of reduction and increment on structural stiffness at nano scales can be considered in the context of NSGT. According to NSGT, two scale factors named nonlocal and strain gradient factors have been utilized to provide an excellent description of small size effects. At first step, it is essential to define the stress field components in the below form (Barati 2018):

$$\sigma_{ij} = \sigma_{ij}^{(0)} - \nabla \sigma_{ij}^{(1)} \tag{1}$$

Note that the symbols $\sigma_{ij}^{(0)}$ and $\sigma_{ij}^{(1)}$ are used for stress components which are respectively associated with strains ε_{kl} and strain gradients $\nabla\varepsilon_{kl}$ as:

$$\sigma_{ij}^{(0)} = \int_V C_{ijkl}\alpha_0(x,x',e_0a)\varepsilon'_{kl}(x')dx' \tag{2a}$$

$$\sigma_{ij}^{(1)} = l^2\int_V C_{ijkl}\alpha_1(x,x',e_1a)\nabla\varepsilon'_{kl}(x')dx' \tag{2b}$$

Here, the symbol C_{ijkl} is used for elastic coefficients; e_0a and e_1a have been used to define the nonlocal effects and l introduces the influences of the strain gradients. If the nonlocal functions $\alpha_0(x,x',e_0a)$ and $\alpha_1(x,x',e_1a)$ can satisfy the introduced conditions by Eringen (1983), the relationship between the stresses and strains in the context of NSGT becomes:

$$\begin{aligned}&[1-(e_1a)^2\nabla^2][1-(e_0a)^2\nabla^2]\sigma_{ij}\\&= C_{ijkl}[1-(e_1a)^2\nabla^2]\varepsilon_{kl}\\&-C_{ijkl}\,l^2[1-(e_0a)^2\nabla^2]\nabla^2\varepsilon_{kl}\end{aligned} \tag{3a}$$

where ∇^2 is called Laplacian operator. The above relation can be more simplified by assuming $e_1a = e_0a = ea$ as:

$$\begin{aligned}&[1-(ea)^2\nabla^2]\sigma_{ij} =\\&C_{ijkl}\,[1-l^2\nabla^2]\varepsilon_{kl}\end{aligned} \tag{3b}$$

2.2. FG materials

The distribution of FG material in structures can be mathematically modeled using power-law or Mori-Tanaka models. Using power-law function, it is possible to easily describe the continuous gradation of material properties with good accuracy, however, Mori-Tanaka scheme has provided more accurate results as reported in some studies. At the first step, assume a FG nano beam with

Table 1 Employed properties of the two phases

Property	Steel	Alumina
E	210 (GPa)	390 (GPa)
ρ	7800 (kg/m^3)	3960 (kg/m^3)
α	13e-6	10.5e-6 (1/K)
ν	0.3	0.24

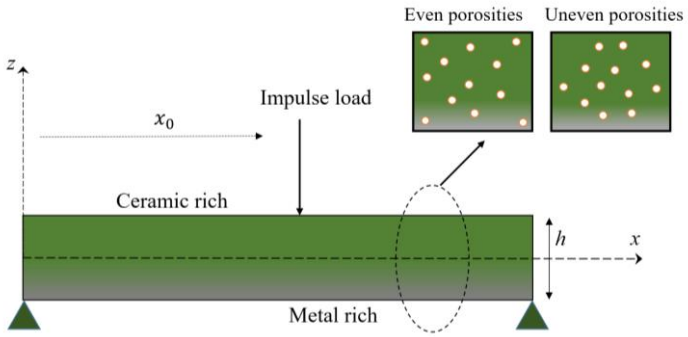

Fig. 1 A pore-dependent graded nanosized beam subjected to an impulse load

length L and thickness h, as indicated in Fig. 1.

Based on power-law functions, it is possible to define Young's modulus (E), Poisson ratio (v), and thermal expansion coefficient (α). Using refined power-law functions, one is potent to model each material property (H) containing porosity volume (ξ) as:

$$H(z)=\left(H_c-H_m\right)\left(\frac{z}{h}+\frac{1}{2}\right)^p+H_m \quad \text{for even distribution} \\ -\left(H_c+H_m\right)\frac{\xi}{2} \tag{4a}$$

$$H(z)=\left(H_c-H_m\right)\left(\frac{z}{h}+\frac{1}{2}\right)^p+H_m \quad \text{for uneven distribution} \\ -\frac{\xi}{2}\left(H_c+H_m\right)\left(1-\frac{2|z|}{h}\right) \tag{4b}$$

Note that p is the material gradient index, It must be stated that the material properties of the metal and ceramic constituents have been presented in Table 1.

2.3. Governing equations

Higher-order beam theories are useful for establishing the governing equations of beams considering shear deformation effect. One of the well-known theories is refined beam theory which has the below form of displacement field (d_x, 0, d_z) as (Issad *et al.* 2018):

$$d_x(x,z) = u(x) - (z-b^*)\frac{\partial w_b}{\partial x} - [B(z)-b^{**}]\frac{\partial w_s}{\partial x} \tag{5a}$$

$$d_z(x,z) = w_b(x) + w_s(x) \tag{5b}$$

The above displacement field contains axial displacement (u); bending displacement (w_b) and shear displacement (w_s). Moreover, in order to determine the neutral axis location in a FG beam, it is necessary to calculate:

$$b^* = \frac{\int_{-0.5h}^{0.5h} E(z)\, z dz}{\int_{-0.5h}^{0.5h} E(z)\, dz} \quad b^{**} = \frac{\int_{-0.5h}^{0.5h} E(z)\, B(z) dz}{\int_{-0.5h}^{0.5h} E(z)\, dz} \tag{6}$$

A trigonometric shear strain function $f(z)$ has been selected as:

$$B(z) = z - \sin(\beta z)/\beta \tag{7}$$

with $\beta = \pi / h$. The derived strains based on the presented displacement field may be introduced as:

$$\varepsilon_{xx} = \frac{\partial u}{\partial x} - (z-b^*)\frac{\partial^2 w_b}{\partial x^2} - [B(z)-b^{**}]\frac{\partial^2 w_s}{\partial x^2} \tag{8a}$$

$$\gamma_{xz} = g(z)\frac{\partial w_s}{\partial x} \tag{8b}$$

Next, the principle of Hamilton based on strain energy (U) and kinetic energy (K) implies that:

$$\int_0^t \delta(U+V-K)\, dt = 0 \tag{9}$$

Also, V introduces the energy of applied forces. The strain energy variation might be introduced by:

$$\delta U = \int_v \sigma_{ij}\delta\varepsilon_{ij}\, dV = \int_v (\sigma_{xx}\delta\varepsilon_{xx} + \sigma_{xx}^{(1)}\delta\nabla\varepsilon_{xx} + \sigma_{xz}\delta\gamma_{xz} + \sigma_{xz}^{(1)}\delta\nabla\gamma_{xz})\, dV \tag{10}$$

Insertion of Eqs. (8a) - (8b) in Eq.(10) leads to:

$$\delta U = \int_0^L (N \frac{\partial \delta u}{\partial x} - M_b \frac{\partial^2 \delta w_b}{\partial x^2} - M_s \frac{\partial^2 \delta w_s}{\partial x^2} + Q \frac{\partial \delta w_s}{\partial x}) dx \tag{11}$$

In such a way that:

$$\begin{aligned} N &= \int_{-h/2}^{h/2} (\sigma_{xx}^0 - \nabla \sigma_{xx}^{(1)}) dz = N^{(0)} - \nabla N^{(1)} \\ M^b &= \int_{-h/2}^{h/2} z(\sigma_{xx}^0 - \nabla \sigma_{xx}^{(1)}) dz = M^{b(0)} - \nabla M^{b(1)} \\ M^s &= \int_{-h/2}^{h/2} f(\sigma_{xx}^0 - \nabla \sigma_{xx}^{(1)}) dz = M^{s(0)} - \nabla M^{s(1)} \\ Q &= \int_{-h/2}^{h/2} g(\sigma_{xz}^0 - \nabla \sigma_{xz}^{(1)}) dz = Q^{(0)} - \nabla Q^{(1)} \end{aligned} \tag{12}$$

where

$$\begin{aligned} N^{(i)} &= \int_{-h/2}^{h/2} (\sigma_{xx}^{(i)}) dz, \\ M^{b(i)} &= \int_{-h/2}^{h/2} z(\sigma_{xx}^{b(i)}) dz, \\ M^{s(i)} &= \int_{-h/2}^{h/2} f(\sigma_{xx}^{s(i)}) dz, \\ Q^{(i)} &= \int_{-h/2}^{h/2} g(\sigma_{xz}^{(i)}) dz, \end{aligned} \tag{13}$$

Note that *i* is 0 or 1. The energy due to the exerted loads might be introduced as follows:

$$\delta V = \int_0^L (q \delta (w_b + w_s)) dx \tag{14}$$

In such a way that:

$$q = +N^T \frac{\partial^2 (w_b + w_s)}{\partial x^2} + f(t) \tag{15}$$

In above relation, *f(t)* is the applied force due to the pulse load. Also, $N^T = \int_{-0.5h}^{+0.5h} \alpha(z) E(z) \Delta T dz$ is the thermal load. A variation on kinetic energy leads to:

$$\begin{aligned} \delta K = \int_0^L (Y_0 [& \frac{\partial u}{\partial t} \frac{\partial \delta u}{\partial t} + (\frac{\partial w_b}{\partial t} + \frac{\partial w_s}{\partial t})(\frac{\partial \delta w_b}{\partial t} \\ & + \frac{\partial \delta w_s}{\partial t})] - Y_1 (\frac{\partial u}{\partial t} \frac{\partial^2 \delta w_b}{\partial x \partial t} + \frac{\partial^2 w_b}{\partial x \partial t} \frac{\partial \delta u}{\partial t}) \\ & + Y_2 (\frac{\partial^2 w_b}{\partial x \partial t} \frac{\partial^2 \delta w_b}{\partial x \partial t}) - J_1 (\frac{\partial u}{\partial t} \frac{\partial^2 \delta w_s}{\partial x \partial t} + \frac{\partial^2 w_s}{\partial x \partial t} \frac{\partial \delta u}{\partial t}) \\ & + S_2 (\frac{\partial^2 w_s}{\partial x \partial t} \frac{\partial^2 \delta w_s}{\partial x \partial t}) + J_2 (\frac{\partial^2 w_b}{\partial x \partial t} \frac{\partial^2 \delta w_s}{\partial x \partial t} \\ & + \frac{\partial^2 w_s}{\partial x \partial t} \frac{\partial^2 \delta w_b}{\partial x \partial t})) dx \end{aligned} \tag{16}$$

where

$$(Y_0, Y_1, J_1, Y_2, J_2, S_2) = \int_{-h/2}^{h/2} \rho\{1, z-b^*, (z-b^*)^2, B-b^{**}, (z-b^*)(B-b^{**}), (B-b^{**})^2\} dz \tag{17}$$

The governing equations have been determined via insertion of Eqs. (11)-(16) in Eq. (9) with setting the coefficients of $\delta u, \delta w_b$ and δw_s to zero:

$$\frac{\partial N}{\partial x} = Y_0 \frac{\partial^2 u}{\partial t^2} - Y_1 \frac{\partial^3 w_b}{\partial x \partial t^2} - J_1 \frac{\partial^3 w_s}{\partial x \partial t^2} \tag{18}$$

$$\frac{\partial^2 M_b}{\partial x^2} - f(t) = +Y_0 \left(\frac{\partial^2 w_b}{\partial t^2} + \frac{\partial^2 w_s}{\partial t^2}\right) + Y_1 \frac{\partial^3 u}{\partial x \partial t^2} - Y_2 \frac{\partial^4 w_b}{\partial x^2 \partial t^2} - J_2 \frac{\partial^4 w_s}{\partial x^2 \partial t^2} + N^T \frac{\partial^2 (w_b + w_s)}{\partial x^2} \tag{19}$$

$$\frac{\partial^2 M_s}{\partial x^2} + \frac{\partial Q}{\partial x} - f(t) = +Y_0 \left(\frac{\partial^2 w_b}{\partial t^2} + \frac{\partial^2 w_s}{\partial t^2}\right) + J_1 \frac{\partial^3 u}{\partial x \partial t^2} - J_2 \frac{\partial^4 w_b}{\partial x^2 \partial t^2} - S_2 \frac{\partial^4 w_s}{\partial x^2 \partial t^2} + N^T \frac{\partial^2 (w_b + w_s)}{\partial x^2} \tag{20}$$

Using Eq. (3), it is possible to establish the stress-strain relations of a higher-order refined FG nano beam in the context of NSGT as:

$$\sigma_{xx} - (ea)^2 \frac{\partial^2 \sigma_{xx}}{\partial x^2} = (1 - l^2 \frac{\partial^2}{\partial x^2}) E(z) \varepsilon_{xx} \tag{21}$$

$$\sigma_{xz} - (ea)^2 \frac{\partial^2 \sigma_{xz}}{\partial x^2} = (1 - l^2 \frac{\partial^2}{\partial x^2}) G(z) \gamma_{xz} \tag{22}$$

Integration from Eqs. (21) and (22) about the nanosized beam thickness leads to the below relations of the forces and moments as:

$$N - (ea)^2 \frac{\partial^2 N}{\partial x^2} = (1 - l^2 \frac{\partial^2}{\partial x^2})(A \frac{\partial u}{\partial x} - B \frac{\partial^2 w_b}{\partial x^2} - B_s \frac{\partial^2 w_s}{\partial x^2}) \tag{23}$$

$$M_b - (ea)^2 \frac{\partial^2 M_b}{\partial x^2} = (1 - l^2 \frac{\partial^2}{\partial x^2})(B \frac{\partial u}{\partial x} - D \frac{\partial^2 w_b}{\partial x^2} - D_s \frac{\partial^2 w_s}{\partial x^2}) \tag{24}$$

$$M_s-(ea)^2\frac{\partial^2 M_s}{\partial x^2}=(1-l^2\frac{\partial^2}{\partial x^2})(B_s\frac{\partial u}{\partial x} -D_s\frac{\partial^2 w_b}{\partial x^2}-H_s\frac{\partial^2 w_s}{\partial x^2}) \tag{25}$$

$$Q-(ea)^2\frac{\partial^2 Q}{\partial x^2}=(1-l^2\frac{\partial^2}{\partial x^2})(A_s\frac{\partial w_s}{\partial x}) \tag{26}$$

where

$$(A,B,B_s,D,D_s,H_s) =\int_{-h/2}^{h/2}E(z)\{1,(z-b^*),(B-b^{**}),(z-b^*)^2,(z-b^*)(B-b^{**}),(B-b^{**})^2\}dz \tag{27}$$

$$A_s=\int_{-h/2}^{h/2}g^2G(z)dz,\ g(z)=1-\partial B(z)/\partial z \tag{28}$$

The established equations with respect to the field components might be represented as follows via the insertion of Eqs. (23)-(26) into Eqs.(18)-(20) as:

$$\begin{aligned}&A(1-l^2\frac{\partial^2}{\partial x^2})(\frac{\partial^2 u}{\partial x^2})-B(1-l^2\frac{\partial^2}{\partial x^2})(\frac{\partial^3 w_b}{\partial x^3})\\&-B_s(1-l^2\frac{\partial^2}{\partial x^2})(\frac{\partial^3 w_s}{\partial x^3})-Y_0\frac{\partial^2 u}{\partial t^2}\\&+Y_1\frac{\partial^3 w_b}{\partial x\partial t^2}+J_1\frac{\partial^3 w_s}{\partial x\partial t^2}+(ea)^2(Y_0\frac{\partial^4 u}{\partial x^2\partial t^2}\\&-Y_1\frac{\partial^5 w_b}{\partial x^3\partial t^2}-J_1\frac{\partial^5 w_s}{\partial x^3\partial t^2})=0\end{aligned} \tag{29}$$

$$\begin{aligned}&B(1-l^2\frac{\partial^2}{\partial x^2})(\frac{\partial^3 u}{\partial x^3})-D(1-l^2\frac{\partial^2}{\partial x^2})(\frac{\partial^4 w_b}{\partial x^4})\\&-D_s(1-l^2\frac{\partial^2}{\partial x^2})(\frac{\partial^4 w_s}{\partial x^4})-Y_0(\frac{\partial^2 w_b}{\partial t^2}+\frac{\partial^2 w_s}{\partial t^2})\\&-Y_1\frac{\partial^3 u}{\partial x\partial t^2}+Y_2\frac{\partial^4 w_b}{\partial x^2\partial t^2}+J_2\frac{\partial^4 w_s}{\partial x^2\partial t^2}\\&+(ea)^2(+Y_0(\frac{\partial^4 w_b}{\partial x^2\partial t^2}+\frac{\partial^4 w_s}{\partial x^2\partial t^2})+Y_1\frac{\partial^5 u}{\partial x^3\partial t^2}\\&-Y_2\frac{\partial^6 w_b}{\partial x^4\partial t^2}-J_2\frac{\partial^6 w_s}{\partial x^4\partial t^2})=f(t)-(ea)^2\frac{\partial^2 f(t)}{\partial x^2}\end{aligned} \tag{30}$$

$$\begin{aligned}&B_s(1-l^2\frac{\partial^2}{\partial x^2})(\frac{\partial^3 u}{\partial x^3})-D_s(1-l^2\frac{\partial^2}{\partial x^2})(\frac{\partial^4 w_b}{\partial x^4})\\&-H_s(1-l^2\frac{\partial^2}{\partial x^2})(\frac{\partial^4 w_s}{\partial x^4})+A_s(1-l^2\frac{\partial^2}{\partial x^2})(\frac{\partial^2 w_s}{\partial x^2})\\&-Y_0(\frac{\partial^2 w_b}{\partial t^2}+\frac{\partial^2 w_s}{\partial t^2})-J_1\frac{\partial^3 u}{\partial x\partial t^2}+J_2\frac{\partial^4 w_b}{\partial x^2\partial t^2}\\&+K_2\frac{\partial^4 w_s}{\partial x^2\partial t^2}+(ea)^2(+Y_0(\frac{\partial^4 w_b}{\partial x^2\partial t^2}+\frac{\partial^4 w_s}{\partial x^2\partial t^2})\\&+J_1\frac{\partial^5 u}{\partial x^3\partial t^2}-J_2\frac{\partial^6 w_b}{\partial x^4\partial t^2}-S_2\frac{\partial^6 w_s}{\partial x^4\partial t^2})=\\&f(t)-(ea)^2\frac{\partial^2 f(t)}{\partial x^2}\end{aligned} \tag{31}$$

The impulse load has been defined as a point load $f(t)=f_0\delta(x-x_0)\Phi(t)$ in which f_0 is

loading amplitude and x_0 is loading location and $\Phi(t)=\sin\left(\frac{\pi t}{t_0}\right)\left(H(t)-H(t-t_0)\right)$.

3. Solution by differential quadrature method (DQM)

In the presented chapter, DQ method has been applied for solving the governing equations for NSGT porous FG nanobeam. According to DQM, at an assumed grid point (x_i, y_j) the derivatives for function F are supposed as weighted linear summation of all functional values within the computation domains as:

$$\frac{d^n F}{dx^n}\Big|_{x=x_i}=\sum_{j=1}^{N} c_{ij}^{(n)} F(x_j) \tag{32}$$

where

$$C_{ij}^{(1)}=\frac{\pi(x_i)}{(x_i-x_j)\ \pi(x_j)} \qquad i,j=1,2,\dots,N, \qquad i\neq j \tag{33}$$

in which $\pi(x_i)$ is defined by

$$\pi(x_i)=\prod_{j=1}^{N}(x_i-x_j), \qquad i\neq j \tag{34}$$

And when $i=j$

$$C_{ij}^{(1)}=c_{ii}^{(1)}=-\sum_{k=1}^{N} C_{ik}^{(1)}, \qquad i=1,2,\dots,N, \qquad i\neq k, \qquad i=j \tag{35}$$

Then, weighting coefficients for high orders derivatives may be expressed by:

$$C_{ij}^{(2)}=\sum_{k=1}^{N} C_{ik}^{(1)}C_{kj}^{(1)},\ C_{ij}^{(3)}=\sum_{k=1}^{N} C_{ik}^{(1)}C_{kj}^{(2)}=\sum_{k=1}^{N} C_{ik}^{(2)}C_{kj}^{(1)}$$

$$C_{ij}^{(4)}=\sum_{k=1}^{N} C_{ik}^{(1)}C_{kj}^{(3)}=\sum_{k=1}^{N} C_{ik}^{(3)}C_{kj}^{(1)} \qquad i,j=1,2,\dots,N. \tag{36}$$

$$C_{ij}^{(5)}=\sum_{k=1}^{N} C_{ik}^{(1)}C_{kj}^{(4)}=\sum_{k=1}^{N} C_{ik}^{(4)}C_{kj}^{(1)},C_{ij}^{(6)}=\sum_{k=1}^{N} C_{ik}^{(1)}C_{kj}^{(5)}=\sum_{k=1}^{N} C_{ik}^{(5)}C_{kj}^{(1)}$$

According to presented approach, the dispersions of grid points based upon Gauss-Chebyshev-Lobatto assumption are expressed as:

$$x_i=\frac{L}{2}\left[1-\cos\left(\frac{i-1}{N-1}\pi\right)\right] \qquad i=1,2,\dots,N, \tag{37}$$

Next, the displacement components may be determined by

$$w_b(x,t)=W_b(x)e^{i\omega t} \tag{38}$$

$$w_s(x,t) = W_s(x)e^{i\omega t} \tag{39}$$

where W_b and W_n denote vibration amplitudes and ω defines the vibrational frequency. Then, it is possible to express obtained boundary conditions as:

$$\begin{aligned} &w_b = w_s = 0, \\ &\frac{\partial^2 w_b}{\partial x^2} = \frac{\partial^2 w_s}{\partial x^2} = 0 \ , \frac{\partial^4 w_b}{\partial x^4} = \frac{\partial^4 w_s}{\partial x^4} = 0 \end{aligned} \tag{40}$$

Now, one can express the modified weighting coefficients for all edges simply-supported as:

$$\begin{aligned} &\bar{C}^{(2)}_{1,j} = \bar{C}^{(2)}_{N,j} = 0, \qquad i = 1, 2, \dots, M, \\ &\bar{C}^{(2)}_{i,1} = \bar{C}^{(2)}_{1,M} = 0, \qquad i = 1, 2, \dots, N. \end{aligned} \tag{41}$$

and

$$\bar{C}^{(3)}_{ij} = \sum_{k=1}^{N} C^{(1)}_{ik} \bar{C}^{(2)}_{kj}, \ \bar{C}^{(4)}_{ij} = \sum_{k=1}^{N} C^{(1)}_{ik} \bar{C}^{(3)}_{kj} \tag{42}$$

Inserting Eqs. (38) - (39) in Eqs. (30)-(31) gives the below relationship:

$$\left\{ [K] + \frac{\partial}{\partial t^2}[M] \right\} \begin{Bmatrix} W_{bn} \\ W_{sn} \end{Bmatrix} = \begin{Bmatrix} f(t) - \mu \dfrac{\partial^2 f(t)}{\partial x^2} \\ f(t) - \mu \dfrac{\partial^2 f(t)}{\partial x^2} \end{Bmatrix} \tag{43}$$

In above equation, [K] and [M] respectively display the stiffness and mass matrices. At the end, with the selection of zero initial conditions and Laplace transform method, Eq. (43) has been re-formulated as:

$$\left\{ [K] + S^2[M] \right\} \begin{Bmatrix} L[W_{bn}] \\ L[W_{sn}] \end{Bmatrix} = \begin{Bmatrix} L[f(t) - \mu \dfrac{\partial^2 f(t)}{\partial x^2}] \\ L[f(t) - \mu \dfrac{\partial^2 f(t)}{\partial x^2}] \end{Bmatrix} \tag{44}$$

By solving Eq.(44) through the inverse Laplace transform approach, one is potent to derive the values of bending (W_{bn}) and shear (W_{sn}) displacements. However, the total deflection of the nanobeam is the summation of the two displacements as $W = W_{bn} + W_{sn}$. For representing the calculated results, the below non-dimension factors have been introduced:

$$t^* = \frac{t}{t_0}, \ \bar{W} = W \frac{100 E_c I}{f_0 L^3}, \ \lambda = \frac{l}{L}, \ \mu = \frac{ea}{L} \tag{45}$$

4. Calculated results and discussion

The present section has been devoted to examine the dynamic responses of porous FG

Table 2 Comparing the non-dimension frequency of a nanaobeam based on NSGT (L/h=20)

		λ=0		λ=0.5	
		Simsek (2019)	Present	Simsek (2019)	Present
p=0	μ =0	2.8491	2.8490	5.3053	5.3051
	μ =0.25	2.2406	2.2406	4.1723	4.1722
	μ =0.5	1.5300	1.5300	2.8491	2.8490
	μ =0.75	1.1130	1.1130	2.0726	2.0724
p=1	μ =0	2.1129	2.1129	3.9345	3.9344
	μ =0.25	1.6617	1.6617	3.0942	3.0942
	μ =0.5	1.1347	1.1346	2.1129	2.1129
	μ =0.75	0.8254	0.8253	1.5371	1.5370

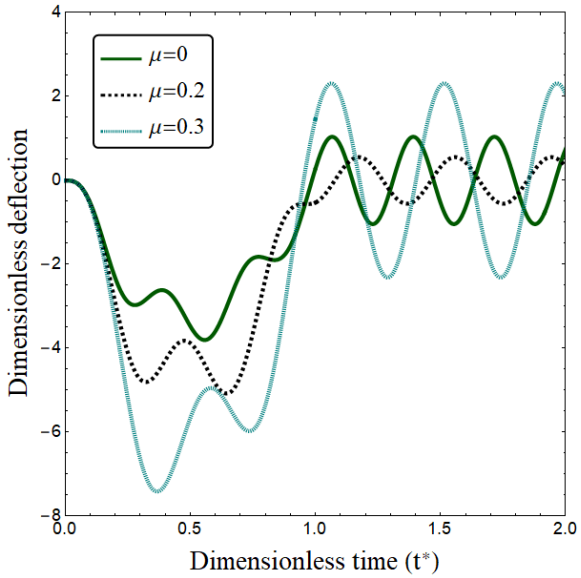

Fig. 2 Time responses of the nanobeam for diverse nonlocality factors (p=1, L=10h, ΔT=20, λ=0, ξ=0.1)

nano beams due to half-sine pulse loads capturing both nonlocal and strain gradient influences. The effects of load location, material gradation, porosity distribution, nonlocality and scale factors on dynamic deflection of the nanobeam have been studied in detail. Within this research, it has been selected that the nonlocality and strain gradient factors are constant for FG nanobeam. Accordingly, μ and λ respectively denote the normalized nonlocal and strain gradient factors. More discussion on this issue can be found in the following paragraphs.

At the first step, a comparison has been provided in Table 2 with the work of Simsek (2019) to validate the vibration frequency of a FG nanobeam based on NSGT. In this regard, the validation of first dimensionless vibration frequency $\Omega = \omega L^2 \sqrt{\rho_c / E_c} / h$, at different values of nonlocal and strain gradient parameters have been carried out and an excellent agreement has been obtained between the obtained results and those of Simsek (2019).

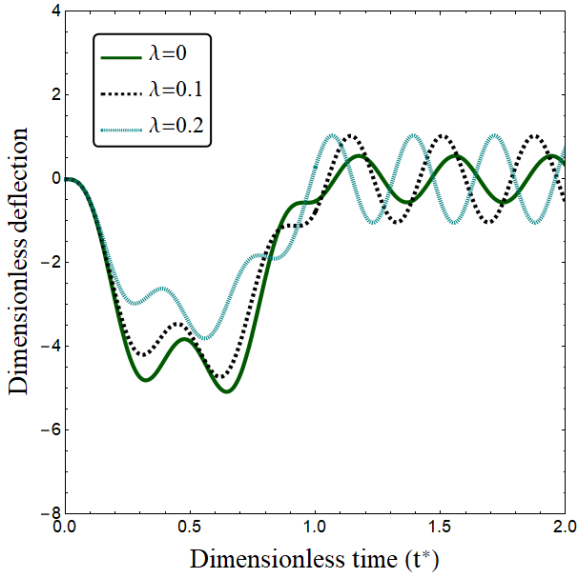

Fig. 3 Time responses of the nanobeam for diverse strain gradient factors (p=1, L=10h, ΔT=20, μ=0.2, ξ=0.1)

Fig. 2 plots the time histories for normalize dynamic deflection at different values of time factor (t^*) and nonlocal parameter (μ=0, 0.2, 0.3) at the FG index p=1. It is assumed in this plot that λ=0 and ΔT=20. In the transient region, an increment in nonlocal factor leads to higher values of normalized dynamic deflection. This is due to reduced stiffness of FGM nanosized beam when the nonlocality factor becomes higher. Such behavior indicates that a FG nanobeam displays stiffness-reducing effects when the nonlocality factor increases.

Dynamic deflection of the nano-size beam against normalized time factor based on different strain gradient factors has been plotted in Fig.3 at p=1 and ΔT=20. For the case of classic elasticity theory (CET), it is assumed that μ= λ=0. Also, it is considered for the case of nonlocality elasticity theory (NET) that μ=0.2 and λ=0. It can be seen that the dynamic deflection is greatly affected by the normalized time. Actually, the dynamic deflection is augmented with the normalized time until reaching peak values, and then it drops abruptly after the points. However, the dynamic deflection and the peak point are dependent on the values of strain gradient factor. Indeed, higher values of strain gradient factor give the lower value of dynamic deflection due to the inclusion of non-unifrom strain field effects. However, by incorporating the strain gradient effect, NSGT gives smaller deflections than NET.

In Fig. 4, the time history of FG nanobeam has been plotted based on various porosity volume fraction (ζ=0, 0.1, 0.2) and FG gradient index (p=1, 3). The even porosity dispersion has been considered for this figure. It can be understood that the FG nanobeam becomes more flexible at a higher value of gradient index because of the higher percentage of metal constituent compared to ceramic constituent. Accordingly, the dynamic deflections of nanobeam increase by increasing the value of gradient index. However, another important factor in dynamic response of a FG nanobeam is the presence of porosities. As the porosity volume (ζ) becomes higher, the value of dynamic deflection becomes higher due to the reason that porosities inside FG material will reduce the structural stiffness.

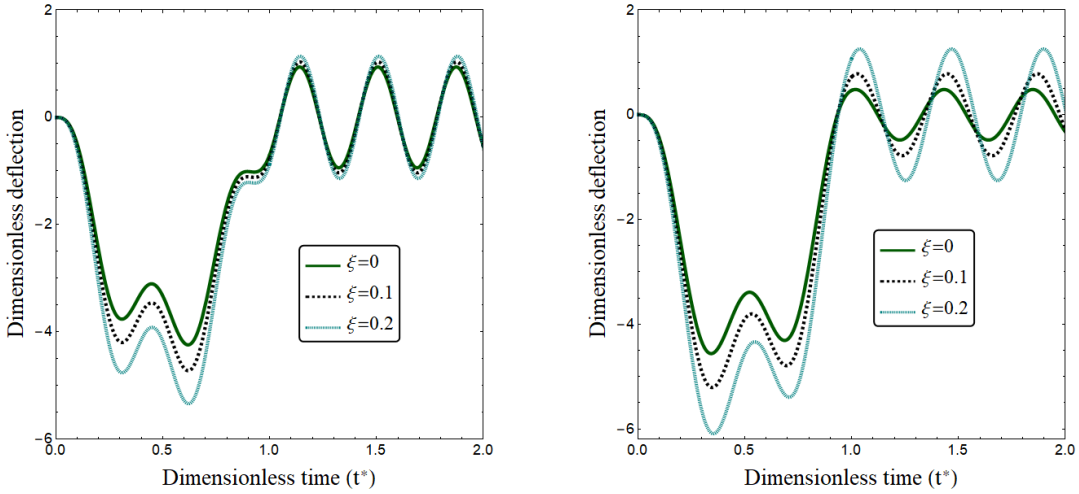

(a) p=1 (b) p=3

Fig. 4 Time responses of the nanobeam for diverse pore factors and material gradient index (L=10h, ΔT=20, μ=0.2, λ=0.1)

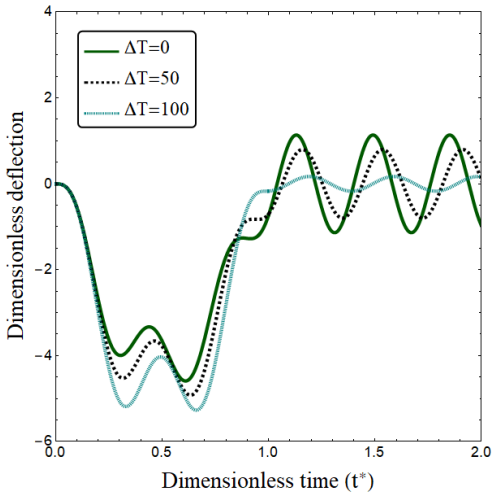

Fig. 5 Time responses of the nanobeam for diverse temperatures (p=1, L=10h, μ=0.2, ξ=0.1)

Dynamic deflection of the nano-size beam against normalized time based on different temperatures (ΔT) has been plotted in Fig. 5 at p=1. In this figure, the nonlocal factor is assumed to be μ= 0.2. It can be seen that the dynamic deflection is greatly affected by the temperature variation. Actually, the dynamic deflection is augmented with the increase of temperature. It means that at higher temperatures, the nanobeam has lower stiffness leading to greater deflections.

A comparison between the dynamic deflection of porous FG nanobeam obtained by even-type and uneven-type porosities has been presented in Fig.6. It is found from this figure that uneven-type porosities give smaller values of dynamic deflection compared with even-type porosities. Actually, the FG nanobeams with even-type porosities are more flexible than uneven-type

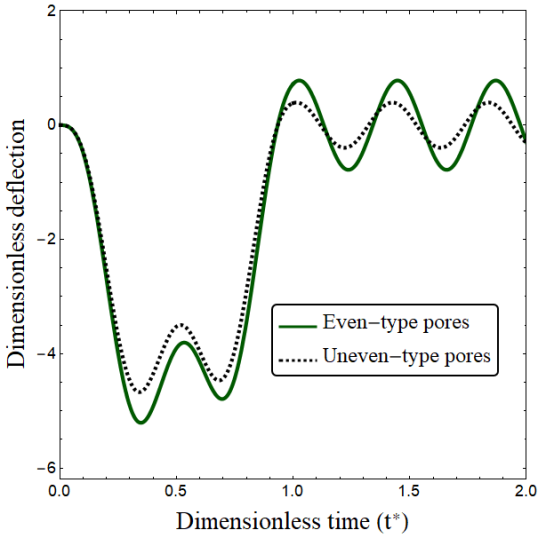

Fig. 6 Time responses of the nanobeam for diverse pore dispersions (p=3, L=10h, μ=0.2, λ=0.1, ξ=0.1, ΔT=20)

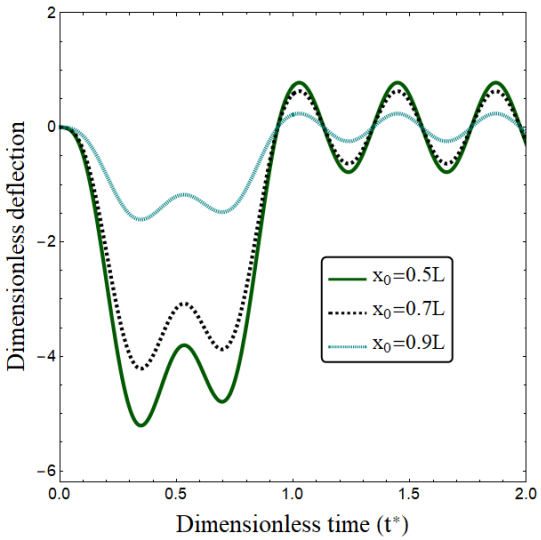

Fig. 7 Time responses of the nanobeam for diverse load location (p=3, L=10h, μ=0.2, λ=0.1, ξ=0.1, ΔT=20)

porosities. The reason is uniform distribution of porosities in cross section area of the FG nanobeam in the case of even model. However, the porosities will not occur at corner of the cross section in the case of uneven model.

Fig.7 displays the effects of loading position (x_0=*0.5L, 0.7L, 0.9L*) on dynamic responses of a FG nano-sized beam exposed to impulse loads when t_0=0.1. It may be concluded from this plot that as the load becomes far from the beam center, the value of normalized deflection in transient region would be lower. Therefore, the maximum value of normalized deflection would be obtained

as the point load is located at the beam center. Another important finding is that the load position has no influecnes on quantity of oscillation in the transient zone.

5. Conclusions

This article dealt with dynamical response invrstigation of a pore-dependent FG nanobeam subjected to a half-sine pulse load considering the effects of nonlocality and strain gradients. A modified power-law model was used to investigate the dynamic characteristics of FG nanobeams including porosity effects. The nanobeam formulation was based upon higher-order refined beam theory, whereas the size effects have been captured according to NSGT. The governing equations were solved using DQM and inverse Laplace transform method. The main findings are summarized as follows:

- An increment in nonlocal factor leads to higher values of normalized dynamic deflection.
- It was reported that NSGT gives smaller deflections than NET.
- The porosity volume becomes higher; the value of dynamic deflection becomes higher due to the reason that porosities inside FG material will reduce the structural stiffness.
- Temperature rise led to higher deflections at transient region.

Acknowledgements

The authors would like to thank Mustansiriyah university (www.uomustansiriyah.edu.iq) Baghdad-Iraq and Middle Technical University (https://www.mtu.edu.iq) for their support in the present work.

References

Ahmed, R.A., Fenjan, R.M. and Faleh, N.M. (2019), "Analyzing post-buckling behavior of continuously graded FG nanobeams with geometrical imperfections", *Geomech. Eng.*, **17**(2), 175-180. https://doi.org/10.12989/gae.2019.17.2.175.

Ahmed, R.A., Fenjan, R.M., Hamad, L.B. and Faleh, N.M. (2020), "A review of effects of partial dynamic loading on dynamic response of nonlocal functionally graded material beams", *Advan. Mater. Res.*, **9**(1), 33-48. https://doi.org/10.12989/amr.2020.9.1.033.

Akgöz, B. and Civalek, Ö. (2015), "A microstructure-dependent sinusoidal plate model based on the strain gradient elasticity theory", *Acta Mechanica*, **226**(7), 2277-2294. https://doi.org/10.1007/s00707-015-1308-4.

Atmane, H.A., Tounsi, A., Bernard, F. and Mahmoud, S.R. (2015), "A computational shear displacement model for vibrational analysis of functionally graded beams with porosities", *Steel Compos. Struct.*, **19**(2), 369-384. https://doi.org/10.12989/scs.2015.19.2.369.

Barati, M.R. (2018), "Vibration analysis of porous FG nanoshells with even and uneven porosity distributions using nonlocal strain gradient elasticity", *Acta Mechanica*, **229**(3), 1183-1196. https://doi.org/10.1007/s00707-017-2032-z.

Ebrahimi, F., Barati, M.R. and Zenkour, A.M. (2018), "A new nonlocal elasticity theory with graded nonlocality for thermo-mechanical vibration of FG nanobeams via a nonlocal third-order shear deformation theory", *Mech. Advan. Mater. Struct.*, **25**(6), 512-522. https://doi.org/10.1080/15376494.2017.1285458.

El-Hassar, S.M., Benyoucef, S., Heireche, H. and Tounsi, A. (2016), "Thermal stability analysis of solar functionally graded plates on elastic foundation using an efficient hyperbolic shear deformation theory", *Geomech. Eng.*, **10**(3), 357-386. https://doi.org/10.12989/gae.2016.10.3.357.

Eltaher, M.A., Emam, S.A. and Mahmoud, F.F. (2012), "Free vibration analysis of functionally graded size-dependent nanobeams," *Appl. Mathem. Comput.*, **218**(14), 7406-7420. https://doi.org/10.1016/j.amc.2011.12.090.

Eringen, A.C. (1983), "On differential equations of nonlocal elasticity and solutions of screw dislocation and surface waves", *J. Appl. Phys.*, **54**(9), 4703-4710. https://doi.org/10.1063/1.332803.

Fenjan, R.M., Ahmed, R.A. and Faleh, N.M. (2021), "Post-buckling analysis of imperfect nonlocal piezoelectric beams under magnetic field and thermal loading", *Struct. Eng. Mech.*, **78**(1), 15-22. https://doi.org/10.12989/sem.2021.78.1.015.

Issad, M.N., Fekrar, A., Bakora, A., Bessaim, A. and Tounsi, A. (2018), "Free vibration and buckling analysis of orthotropic plates using a new two variable refined plate theory", *Geomech. Eng.*, **15**(1), 711-719. https://doi.org/10.12989/gae.2018.15.1.711.

Khaniki, H.B. and Hosseini-Hashemi, S. (2017), "The size-dependent analysis of multilayered microbridge systems under a moving load/mass based on the modified couple stress theory", *Europ. Phys. J. Plus*, **132**(5), 200. https://doi.org/10.1140/epjp/i2017-11466-0.

Kunbar, L.A.H., Hamad, L.B., Ahmed, R.A. and Faleh, N.M. (2020), "Nonlinear vibration of smart nonlocal magneto-electro-elastic beams resting on nonlinear elastic substrate with geometrical imperfection and various piezoelectric effects", *Smart Struct. Syst.*, **25**(5), 619-630. https://doi.org/10.12989/sss.2020.25.5.619.

Lam, D.C., Yang, F., Chong, A.C.M., Wang, J. and Tong, P. (2003), "Experiments and theory in strain gradient elasticity", *J. Mech. Phys. Solids*, **51**(8), 1477-1508. https://doi.org/10.1016/S0022-5096(03)00053-X.

Li, L., Hu, Y. and Ling, L. (2015), "Flexural wave propagation in small-scaled functionally graded beams via a nonlocal strain gradient theory", *Compos. Struct.*, **133**, 1079-1092. https://doi.org/10.1016/j.compstruct.2015.08.014.

Liu, H., Zhang, Q. and Ma, J. (2021), "Thermo-mechanical dynamics of two-dimensional FG microbeam subjected to a moving harmonic load", *Acta Astronautica*, **178**, 681-692. https://doi.org/10.1016/j.actaastro.2020.09.045.

Lou, J., He, L., Wu, H. and Du, J. (2016), "Pre-buckling and buckling analyses of functionally graded microshells under axial and radial loads based on the modified couple stress theory", *Compos. Struct.*, **142**, 226-237. https://doi.org/10.1016/j.compstruct.2016.01.083.

Martínez-Criado, G. (2016), "Application of micro-and nanobeams for materials science", *Synchrotron light sources and free-electron lasers: accelerator physics, instrumentation and science applications,* 1505-1539. https://doi.org/10.1007/978-3-319-14394-1_46.

Mirjavadi, S.S., Bayani, H., Khoshtinat, N., Forsat, M., Barati, M.R. and Hamouda, A.M.S. (2020a), "On nonlinear vibration behavior of piezo-magnetic doubly-curved nanoshells", *Smart Struct. Syst.*, **26**(5), 631-640. https://doi.org/10.12989/sss.2020.26.5.631.

Mirjavadi, S.S., Forsat, M., Yahya, Y.Z., Barati, M.R., Jayasimha, A.N. and Hamouda, A.M.S. (2020b), "Porosity effects on post-buckling behavior of geometrically imperfect metal foam doubly-curved shells with stiffeners", *Struct. Eng. Mech.*, **75**(6), 701-711. https://doi.org/10.12989/sem.2020.75.6.701.

Nami, M.R. and Janghorban, M. (2014), "Resonance behavior of FG rectangular micro/nano plate based on nonlocal elasticity theory and strain gradient theory with one gradient constant", *Compos. Struct.*, **111**, 349-353. https://doi.org/10.1016/j.compstruct.2014.01.012.

She, G.L., Yuan, F.G., Ren, Y.R., Liu, H.B. and Xiao, W.S. (2018), "Nonlinear bending and vibration analysis of functionally graded porous tubes via a nonlocal strain gradient theory", *Compos. Struct.*, **203**, 614-623. https://doi.org/10.1016/j.compstruct.2018.07.063.

Şimşek, M. (2010), "Dynamic analysis of an embedded microbeam carrying a moving microparticle based on the modified couple stress theory", *Int. J. Eng. Sci.*, **48**(12), 1721-1732. https://doi.org/10.1016/j.ijengsci.2010.09.027.

Şimşek, M. (2019), "Some closed-form solutions for static, buckling, free and forced vibration of functionally graded (FG) nanobeams using nonlocal strain gradient theory", *Compos. Struct.*, **224**, 111041. https://doi.org/10.1016/j.compstruct.2019.111041.

Zhang, B., He, Y., Liu, D., Shen, L. and Lei, J. (2015), "Free vibration analysis of four-unknown shear deformable functionally graded cylindrical microshells based on the strain gradient elasticity theory", *Compos. Struct.*, **119**, 578-597. https://doi.org/10.1016/j.compstruct.2014.09.032.

Zhang, Q. and Liu, H. (2020), "On the dynamic response of porous functionally graded microbeam under moving load", *Int. J. Eng. Sci.*, **153**, 103317. https://doi.org/10.1016/j.ijengsci.2020.103317.

CC